microbial biotechnology

Open Access

# A polyhydroxyalkanoates bioprocess improvement case study based on four fed-batch feeding strategies

**Maciej W. Guzik,[1,2] Gearóid F. Duane,[3] Shane T. Kenny,[1] Eoin Casey,[3] Paweł Mielcarek,[4] Magdalena Wojnarowska[5] and Kevin E. O'Connor[1]**

[1]*School of Biomolecular and Biomedical Sciences and BiOrbic Bioeconomy SFI Research Centre, UCD O'Brien Centre for Science, University College Dublin, Belfield, Dublin 4, Ireland.*

[2]*Jerzy Haber Institute of Catalysis and Surface Chemistry Polish Academy of Sciences, Niezapominajek 8, Kraków, 30-239, Poland.*

[3]*School of Chemical and Bioprocess Engineering, Engineering and Materials Science Centre, University College Dublin, Belfield, Dublin 4, Ireland.*

[4]*Department of Organizational Theory and Management, Poznań University of Economics and Business, al. Niepodległości 10, Poznań, 61-875, Poland.*

[5]*Department of Product Technology and Ecology, Cracow University of Economics, ul. Rakowicka 27, Kraków, 31-510, Poland.*

## Summary

**The modelling and optimization of a process for the production of the medium chain length polyhydroxyalkanoate (mcl-PHA) by the bacterium *Pseudomonas putida* KT2440 when fed a synthetic fatty acid mixture (SFAM) was investigated. Four novel feeding strategies were developed and tested using a constructed model and the optimum one implemented in further experiments. This strategy yielded a cell dry weight of 70.6 g $l^{-1}$ in 25 h containing 38% PHA using SFAM at 5 l scale. A phosphate starvation strategy was implemented to improve PHA content, and this yielded 94.1 g $l^{-1}$ in 25 h containing 56% PHA using SFAM at 5 l scale. The process was successfully operated at 20 l resulting in a cell dry weight of 91.2 g $l^{-1}$ containing 65% PHA at the end of a 25-h incubation.**

Received 14 March, 2021; revised 10 June, 2021; accepted 18 June, 2021.
For correspondence. E-mail kevin.oconnor@ucd.ie; Tel. +353 1 716 2198; Fax +353 1 716 1183.
We dedicate this manuscript to our friend Dr Shane T. Kenny, who sadly left us too early.
*Microbial Biotechnology* (2022) **15**(3), 996–1006
doi:10.1111/1751-7915.13879

## Introduction

With increased mechanistic understanding of biosynthesis, new opportunities for the production of polymers from renewable resources arise (Babu *et al.*, 2013; Guzik *et al.*, 2020). Biopolymers are synthesized by enzymes that link building blocks such as amino acids, sugars or hydroxy fatty acids to yield high molecular weight molecules (Moradali and Rehm, 2020). Polyhydroxyalkanoates (PHA) are examples of bioplastics consisting of polyesters of various hydroxyalkanoic acids and are synthesized by numerous microorganisms. Bioplastics can be seen as alternatives to conventional petrochemical plastics due to their biodegradability and their derivation from renewable resources (Guzik *et al.*, 2020). Moreover, the utilization of wastes as substrates for bioconversion into bio-based plastic is one of the strategies of the European Bioeconomy (Drzyzga *et al.*, 2015). There are several areas where further research is needed for viable PHA production. For instance, there is optimization needed in terms of cost of used substrate (Dias *et al.*, 2006; Salmiati *et al.*, 2007), types and methods of fermentation (Fournet *et al.*, 2020), impact of bioplastic on human health (Moradali and Rehm, 2020) or their effects on environmental sustainability (Narancic *et al.*, 2018; Nitkiewicz *et al.*, 2020).

With the above in mind, the present research aims to fill the knowledge gap on model-based optimization of the fed-batch bioprocesses for PHA production form fatty acids. The first step is a determination of biological conditions for the bacterial growth, feeding and fermentation process. Next, a focus is put on the development of mathematical model for fed-batch feeding and the optimization of the fermentation process. This holistic approach allows formulation of conclusions, both in terms of modelling of the most efficient feeding and fermentation strategy in order to obtain PHA polymer, as well as in terms of identification of the key variables that determine improvement of the production process. The approach presented here, based on mathematical and statistical methods is an improvement over 'trial-and-error' learning processes (Baldassarre *et al.*, 2017).

We examined the modelling and optimization of the production of medium chain polyhydroxyalkanoate (mcl-PHA) by the bacterium *Pseudomonas putida* KT2440 with a mixture of fatty acids as feedstock. The synthetic fatty acid mixture (SFAM) contained both odd and even

carboxylic acids ranging from butanoic to tetradecanoic acids in order to produce a mcl-PHA that potentially can be used in bio-adhesive formulations. Novel feeding strategies were developed and tested using a constructed model and the optimum one implemented in the 20-litre experiment.

## Results and discussion

### *Determination of basic fermentation parameters*

Batch and initial fed-batch fermentation experiments (data not shown) were performed in order to determine the basic model parameters (Table 1). The parameter values compared very well to literature values seen for similar systems using single fatty acid substrates (Lee *et al*., 2000; Hartmann *et al*., 2006; Maclean *et al*., 2008). No previous study has used such a broad mixture of fatty acids for growth of bacteria. The value of the maximum specific growth rate of 0.45 $h^{-1}$ is identical to that stated for the growth of *P. putida* KT2440 on nonanoic acid (Maclean *et al*., 2008). The yield coefficient of biomass on the mixed fatty acids (SFAM) substrate of 0.8 g $g^{-1}$ was also very similar to that obtained (0.83 g $g^{-1}$) for *P. putida* KT2440 grown on a single fatty acid (nonanoic acid) (Sun *et al*., 2007). The yield coefficient of biomass on oxygen ($Y_{X/O}$) of 1.5 g $g^{-1}$ was estimated initially using a stoichiometric balance and later confirmed using the bank of fed-batch data as the oxygen mass transfer coefficient was known. There were no values found for directly comparable systems in the literature with regard to $Y_{X/O}$, but the value of 1.25 g $g^{-1}$ found for *P. putida* IPT046 grown on glucose compares favourably (Cardoso Diniz *et al*., 2004). The yield coefficient of biomass on inorganic phosphate of 61.0 g $g^{-1}$ was very similar to that of 63.4 g $g^{-1}$ seen for *P. putida* KT2440 grown on nonanoic acid (Sun *et al*., 2007). The yield of biomass on ammonium of 9.0 g $g^{-1}$ compared well to the range of values (9.1 g $g^{-1}$) found for *P. putida* $GPo^{-1}$ grown on a mixture of octanoic and 10-undecenoic acid in chemostat culture under various dilution rates (Hartmann *et al*., 2006).

**Table 1.** Basic fermentation parameters established for the investigated system.

| Parameter | Unit | Value |
|---|---|---|
| $\mu_{max}$ | $h^{-1}$ | 0.45 ± 0.02 |
| $Y_{X/S}$ | g $g^{-1}$ | 0.80 ± 0.05 |
| $Y_{X/O}$ | g $g^{-1}$ | 1.5 ± 0.1 |
| $Y_{X/NH4}$ | g $g^{-1}$ | 9.0 ± 1.0 |
| $Y_{X/P}$ | g $g^{-1}$ | 61.0 ± 3.0 |
| $K_S$ | mol $l^{-1}$ | $5.0 \times 10^{-4}$ |
| $k_La$ | $s^{-1}$ | Varies[a] |

**a**. $k_La$ varies based on the fermentor used (Biostat B+ vs. Biostat C+ system); time of the fermentation and also it decreases as the cell density increases.

### *Simple exponential feeding*

First, an exponential feeding regime was employed due to its simplicity and to investigate the system's maximum cell generation rate and confirm the oxygen transfer capacity of the reactor. The aim was to maintain a constant specific growth rate until the biological oxygen demand exceeded the physical supply, and the experiment was ended by oxygen limitation. This would give information about the maximum cell generation rate ($\mu X$) that could be achieved for this system, which would help inform later experiments.

A conservative constant specific growth rate of 0.25 $h^{-1}$ (Fig. 1) was chosen to prevent substrate overfeeding (μ maximum is 0.45 $h^{-1}$). The resulting experimental constant specific growth rate was 0.22 $h^{-1}$. A total of 28.1 g $l^{-1}$ of biomass with 33% of that biomass accumulated as PHA (9.2 g $l^{-1}$) within 19 h. The fermentation ended due to oxygen limitation, which caused SFAM accumulation and resulted in uncontrollable foaming. This allowed the calculation of μX, which reached a maximum of 6.3 g $l^{-1}$ $h^{-1}$ and was seen to be considerably lower than the 14 g $l^{-1}$ $h^{-1}$ achieved for *P. putida* KT2440 grown on nonanoic acid (Maclean *et al*., 2008). This was expected, however, as Maclean *et al*. (2008) supplemented the air flow with pure oxygen (up to 100% pure oxygen) in order to maintain the dissolved oxygen levels in the reactor and reach higher cell densities.

### *Model accuracy*

As can be seen in Fig. 1 (constant exponential specific growth rate), there is excellent agreement between the predicted results from the model and the experimental data. This gave confidence in the validity of the model and its usefulness as a predictive tool. As such, it was deemed suitable to use the model as a predictive tool to test new feeding strategies for their potential to improve process performance. Out of this work came a novel feeding strategy that was then employed experimentally.

### *SFAM feeding based on a linearly and a quadratically decaying specific growth rates*

Two feeding strategies developed by Maclean *et al*. (2008) were applied to our system. First, a linearly decaying specific growth rate was imposed on the *P. putida* KT2440 fermentation using SFAM (referred to as 'Linear' profile). After the initial 9 h of controlled exponential feeding ($\mu = 0.25\ h^{-1}$), the system achieved

 

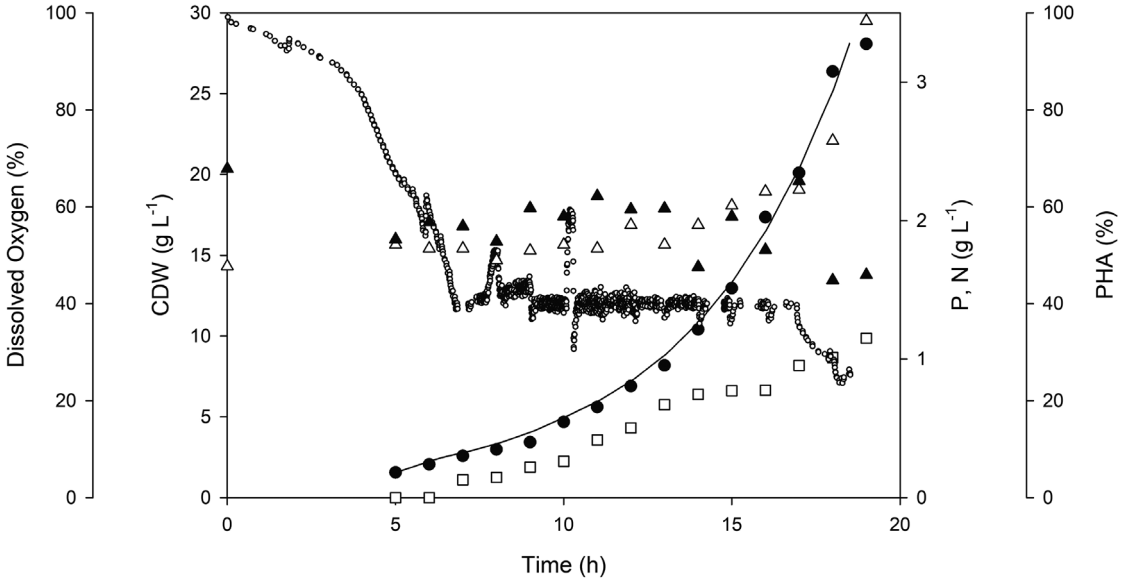


**Fig. 1.** Growth of *P. putida* KT2440 supplied with SFAM that was fed exponentially to control growth rate (μ) at 0.25 h$^{-1}$ (referred to as 'Pure exponential' profile). Cell dry weight (CDW) (g l$^{-1}$, ●), PHA concentration (%, □), phosphorus concentration ($g_P$ l$^{-1}$, ▲), nitrogen concentration ($g_N$ l$^{-1}$, △) and dissolved oxygen (%, ○) were tracked over time. The experimental data were compared to model predictions (corresponding lines).

4.4 g l$^{-1}$ of biomass. This was the starting point of the imposed linearly decaying specific growth rate feeding regime. The parameters for Equations 2–4 were set at $\mu_{init}$ = 0.25 h$^{-1}$ and $t_{max}$ = 40 h. This ensured the system would never achieve a greater μX than 6.0 g l$^{-1}$ h$^{-1}$. The specific growth rate linearly fell from 0.25 h$^{-1}$ to approximately 0.10 h$^{-1}$ by the end of the fermentation. SFAM was the only limiting factor throughout the fermentation.

A total of 71.3 g l$^{-1}$ biomass were accumulated within 27 h, which corresponds to a biomass volumetric productivity of 2.6 g l$^{-1}$ h$^{-1}$ (Fig. S3). The fermentation ended after 27 h due to oxygen limitation, which as previously observed resulted in fatty acid accumulation and subsequent foaming. The fermentation with SFAM ended earlier than that reported by Maclean *et al*. (2008), using a single fatty acid, i.e. nonanoic acid. Furthermore, cells supplied with SFAM accumulated 1.27-fold lower biomass compared to cells grown by Maclean *et al*. (2008) on nonanoic acid. PHA reached 47% of a total biomass which is 1.38-fold lower PHA content compared to the cells supplied with nonanoic acid (Maclean *et al*., 2008).

In the second approach, we have tested the quadratically decaying specific growth rate fermentation strategy earlier developed for nonanoic acid and *P. putida* KT2440 (referred to as 'Quadratic' profile). The SFAM concentration in the fermentor at time of inoculation was 1 g/l (0.84 $g_C$ l$^{-1}$). The culture grew at $\mu_{max}$ initially (0–5 h) which was set as 0.45 h$^{-1}$ in Equations 5–7. After 5 h, the SFAM was fed according to the quadratic model[31] for the next 10 h, which was followed by a constant feed until the end of the fermentation.

This strategy allowed the shortening of the fermentation run to 24 h, while attaining a high biomass level of 73.4 g l$^{-1}$, which corresponds to a biomass productivity of 3.1 g l$^{-1}$ h$^{-1}$ (Fig. S4). PHA levels at the end of the fermentation were 42% of the cell dry weight (1.3 g l$^{-1}$ h$^{-1}$). The run was ended in a similar manner to the previous runs by oxygen limitation. When compared to the results obtained by Maclean and *et al*. (2008), it was visible that composition of our substrate (SFAM) plays a significant role on the system performance. First, our run finished at 24 h, while the nonanoic feed reported by Maclean *et al*. (2008) allowed for operation past 30 h mark using oxygen enriched air. Second, as was observed for the linearly decaying specific growth rate feeding profile, overall system productivity using SFAM was lower than that reported by Maclean and colleagues on nonanoic acid (109 g l$^{-1}$ of CDW with 63% PHA) but the volumetric productivity was very similar (2.4 g PHA l$^{-1}$ h$^{-1}$).

### *A novel feeding strategy developed for a fatty acid mixture*

Based of the above observations and being aware of our system behaviour in presence of the complex mixture of fatty acids, a hybrid strategy was developed. This strategy is a combination of an exponential feeding of a substrate to a certain time point, where an exponentially decaying specific growth rate feeding regime is imposed

 

in order to maximize the process yields. Application of this feeding pattern allowed operation for 25 h. The increase of biomass during the first 11 h was significantly higher than that achieved with the previous feeding strategy (quadratically decaying specific growth rate), reaching a 2.2-fold higher CDW. However, after this point, the accumulation rate slowed down and equalled the previous feeding profile. At time 25 h, the dissolved oxygen level in the reactor became limiting, fatty acids started to accumulate, cell lysis and foaming was observed and finally termination of the fermentation occurred. A total of 70.5 g $l^{-1}$ of cell dry weight were accumulated within 25 h resulting in an overall productivity of 2.8 g $l^{-1}$ $h^{-1}$ (Fig. 2). PHA was accumulated to a level of 36%, giving 1.0 g $l^{-1}$ $h^{-1}$ of overall PHA volumetric productivity (Fig. 2).

While the cell dry weight achieved with SFAM compared well to that achieved by Maclean, *et al*. (2008) (~ 87 g $l^{-1}$ in 25 h using nonanoic acid), the PHA content was significantly lower. As a result, the total PHA productivity of the experiment was significantly lower than Maclean, *et al.,* who achieved 2.3 g $l^{-1}$ $h^{-1}$ after 30 $h^{-1}$. This higher productivity may be due to the oxygen enriched air feeding strategy employed by Maclean *et al*. (2008). At 5 l scale, we achieved significantly lower cell dry weight than Lee, *et al*. (141 g $l^{-1}$ in 38 h) who used oleic acid and oxygen enriched air. Lee *et al*. (2000) reported 53% of the cell dry weight as PHA and thus had a PHA productivity of 1.91 g $l^{-1}h^{-1}$ (almost double our PHA productivity). However, as you will see in the next section, we significantly increased the biomass and PHA productivity in the 20 l reactor using phosphate limitation and without the use of oxygen enriched air.

### *Increasing levels of PHA by imposing inorganic phosphate starvation*

It was seen that in order to enhance PHA productivity, a higher PHA content per cell would be required. Lee *et al*. (2000) successfully imposed inorganic phosphate limitation to increase the PHA content of the cells supplied with oleic acid. Based on this information, an inorganic phosphate starvation strategy was designed for the synthetic fatty acids mixture (SFAM). The model was used to calculate the required inorganic phosphate feed so that phosphate starvation would occur at hour 20. This time point was chosen for a number of reasons. First, there was a significantly large cell dry weight accumulated at this time (~50 g $l^{-1}$). Second, there was still a significant dissolved oxygen level present in the reactor, which would allow cells to remain viable for an extended PHA accumulation phase. Finally, it was envisaged that imposing phosphate starvation at this time point would prolong PHA accumulation and increase the PHA content of cells (consult Fig. S5 for difference between non-limiting and limiting conditions). We observed that the PHA accumulation rate was exponential up to 13 h after which the rate of PHA accumulation decreased (Fig. 2) and the PHA content of the cells remained constant (~ 35% of CDW) over the remainder of the fermentation.

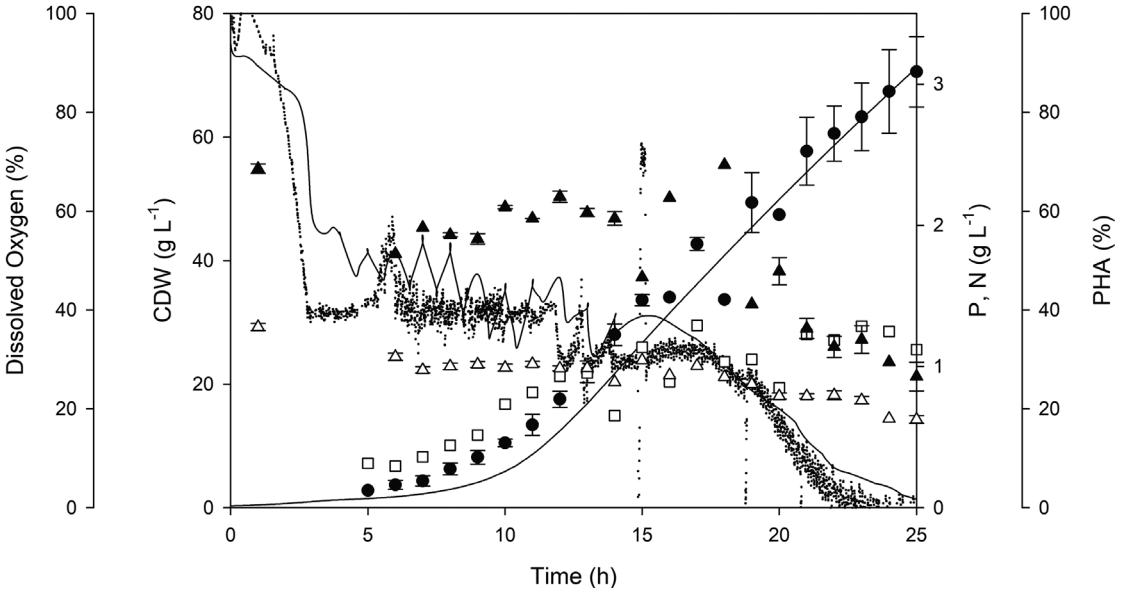


**Fig. 2.** Growth of *P. putida* KT2440 on SFAM fed according to a novel feeding strategy (referred to as 'Novel' profile). Cell dry weight (CDW) (g $l^{-1}$, ●), PHA concentration (%, □), phosphorus concentration ($g_P$ $l^{-1}$, ▲), nitrogen concentration ($g_N$ $l^{-1}$, △) and dissolved oxygen (%, ○) were tracked over time. The experimental data were compared to model predictions (corresponding lines).

 

Based on the mathematical model prediction of the time when the phosphate concentration would become limiting, the initial concentration of phosphate in the growth medium was changed from 2.50 $g_P$ $l^{-1}$ to 1.03 $g_P$ $l^{-1}$ (Fig. 3). This resulted in the accumulation of 94.1 g $l^{-1}$ of dry biomass in 25 h, which translated to an overall volumetric productivity of 3.8 g $l^{-1}$ $h^{-1}$. PHA accumulated at time 25 h reached a level of 56% corresponding to a volumetric productivity of 2.1 g $l^{-1}$ $h^{-1}$. Once again, the fermentation ended due to dissolved oxygen limitation and the associated fatty acid accumulation. The excellent agreement between the model and experimental data highlighted the accuracy and capability of the model as it removed the need for trial-and-error experimentation in order to find the correct inorganic phosphate level required.

When phosphate limitation was imposed at time 20 h, the system was able to accumulate biomass for a further 5 h with no detectable phosphorous present in the media. This may be due to inorganic phosphate conversion to polyphosphate earlier in the growth cycle, as previously reported for *P. putida* KT2440 (Tobin *et al.*, 2007), which would enable further growth until the bacteria ran out of phosphate reserve. The 1.5-fold increase in PHA content from 36% to 56% shows the value of phosphate starvation as a means to improve the total PHA content of the cells for this system and hence total PHA productivity.

These results proved the value of the modelling exercise as it resulted in improved process performance without the need for the addition of expensive oxygen to the air supply. Furthermore, it also significantly reduced the experimental workload that is required in traditional 'trial-and-error' process improvement.

### *Bioprocess transfer from 5 to 20 l working volume*

The novel feeding strategy was deemed successful, and accordingly, it was transferred from the Biostat B+ (5 l working volume) to Biostat C+ (20 l working volume) fermentor. As the geometry and mass transfer characteristics of the Biostat C+ fermenter are similar to those of the Biostat B+, it was assumed that growth would be similar in the larger fermenter. Thus, everything (inoculum, feed rates, etc.) was scaled fourfold. Using a phosphate limitation strategy, the biomass level was slightly lower in the larger fermentor compared to that obtained at smaller scale but there was an increase in PHA accumulation, which reached 65% of CDW at 20 l scale, which translates to an overall PHA volumetric productivity of 2.4 g $l^{-1}$ $h^{-1}$ (Table 2) which matches the 2.3 g $l^{-1}$ $h^{-1}$ PHA productivity reported by Maclean *et al.* (2008) using nonanoic acid and oxygen enriched air.

### *Mcl-PHA polymer*

Throughout the course of the model development and process improvement, the monomer composition of the mcl-PHA obtained did not vary significantly between the different feed profiles (Table S1). The polymer composition

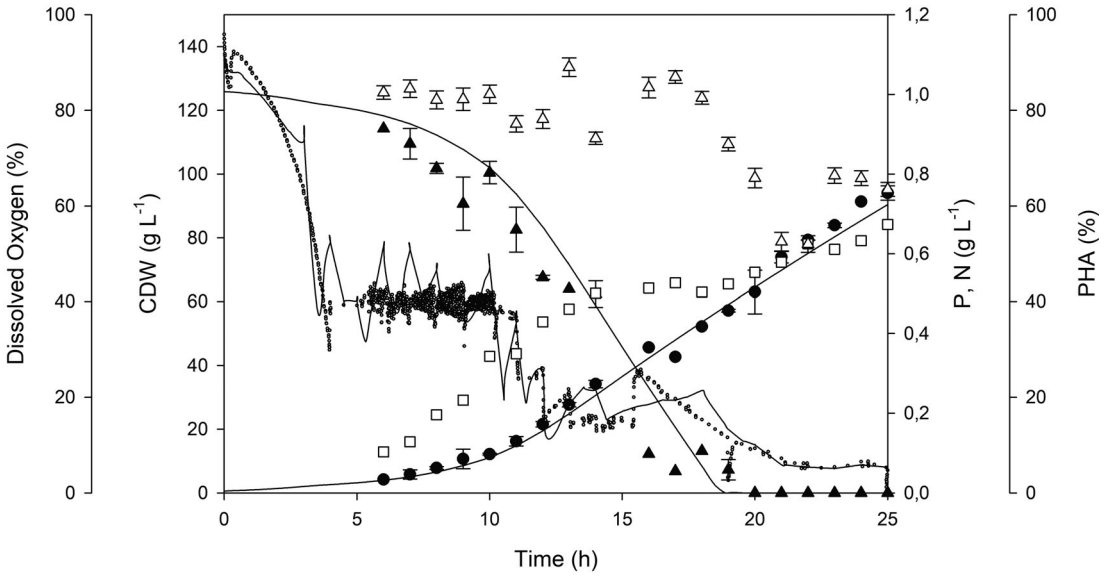


**Fig. 3.** Growth of *P. putida* KT2440 on SFAM fed according to a novel feeding strategy with inorganic phosphate starvation imposed from hour 20 to the end (referred to as 'Novel, Plim' profile). Cell dry weight (CDW) (g $l^{-1}$, ●), PHA concentration (%,□), phosphorus concentration ($g_P$ $l^{-1}$, ▲), nitrogen concentration ($g_N$ $l^{-1}$, △) and dissolved oxygen (%, ○) were tracked over time. The experimental data were compared to model predictions (corresponding lines).

 

**Table 2.** Growth and PHA accumulation of *P. putida* KT2440 during the course of model development and process improvement.

| Fermentation | Fermentor | Time [h] | CDW [g $l^{-1}$] | PHA [%] | PHA [g $l^{-1}$] | Vol. prod. CDW [g $l^{-1}$ $h^{-1}$] | Vol. prod. PHA [g $l^{-1}$ $h^{-1}$] |
|---|---|---|---|---|---|---|---|
| Pure exponential | Biostat B+ (5 l) | 19 | 28.1 | 33 | 9.2 | 1.5 | 0.5 |
| Linear | Biostat B+ (5 l) | 27 | 71.3 | 47 | 33.8 | 2.6 | 1.3 |
| Quadratic | Biostat B+ (5 l) | 24 | 73.4 | 42 | 31.1 | 3.1 | 1.3 |
| Novel | Biostat B+ (5 l) | 25 | 70.6 | 38 | 26.0 | 2.8 | 1.0 |
| Novel, Plim | Biostat B+ (5 l) | 25 | 94.1 | 56 | 52.8 | 3.8 | 2.1 |
| Novel, Plim | Biostat C+ (20 l) | 25 | 91.2 | 65 | 59.4 | 3.6 | 2.4 |

corresponded closely to the substrate fed and contained both odd and even saturated monomer units. The predominant monomers were 3-hydroxyoctanoate (avg 27 mol%) and 3-hydroxynonanoate (avg 24 mol%), followed by 3-hydroxyheptanoate (avg 17 mol%) and 3-hydroxydecanoate (avg 16 mol%). The remaining monomers yielded below 10 mol% each and consisted of 3-hydroxyhexanoate (avg 7 mol%), 3-hydroxyundecanoate (avg 6 mol%), 3-hydroxydodecanoate (avg 3 mol%) and 3-hydroxytridecanoate (avg 1 mol%). The extracted polymer was runny, very sticky in touch and slightly yellow in colour. These characteristics suggest it can be a very promising bio-adhesive additive; however, further investigations in the processing and performance of the polymer in the future are needed.

### *Statistical validation of the process*

According to abovementioned different fermentation and feeding strategies, one of crucial areas of analysis is to recognize which one of different fermentation methods is the most efficient in terms of achieving CDW [g $l^{-1}$] and PHA [%] for a manufacturing process implementation. Therefore, a twostep procedure was applied. The first phase aimed to determine the most efficient feeding strategy based on regression models. The second phase was focussed on diagnosis of relationships between each of variables within most efficient feeding strategy. In order to achieve this, several statistical methods were used. Among them are the correlation coefficient of variables and Cronbach's alpha test.

In the first step of verification, a regression model was applied. This method presents efficiency of growth of CDW and PHA with coefficient: $R^2$ adjusted (further as $R^2_{adj.}$). All models were calculated based on *P*-value = 0.05. Fourth column of the Table 3 presents average value of $R^2_{adj.}$ of CDW and PHA. This metric can be interpreted as aggregated synthetic score showing efficiency of the feeding strategy. Because both dependent variables (CDW and PHA) are treated as equally valuable as a result of experiment. That is why the closer the value of the fourth column to 1, the more CDW and PHA increased with time. According to above dependencies, the most efficient growth strategy is 20 l Novel Plim with $R^2_{adj.}$ = 98.35%. For most efficient

**Table 3.** Regression models for fermentation and feeding strategies according to CDW [g $l^{-1}$] and PHA [%] results.

| | $R^2$ adjusted | | | Standard deviation | |
|---|---|---|---|---|---|
| Fermentation and feeding strategy | CDW [g $l^{-1}$] | PHA [%] | Average value of $R^2_{adj.}$ of CDW & PHA | CDW [g $l^{-1}$] | PHA [%] |
| Linear SFAM | 90.50% | 92.40% | 91.45% | 7.14436 | 0.041308 |
| Quadratic SFAM | 97.10% | 76.10% | 86.60% | 4.1309 | 0.065162 |
| Novel | 97.20% | 78.20% | 87.70% | 3.85274 | 0.047092 |
| Novel Plim | 97.90% | 89.70% | 93.80% | 4.44706 | 0.046544 |
| 20 l Novel Plim | 98.90%[a] | 97.80%[b] | 98.35% | 3.33829 | 2.8207 |
| Feeding strategy with Phosphorous as a stress factor | | | | | |
| Novel Plim | 98.38% | 92.21% | 95.30% | 4.03325 | 0.0415534 |
| 20 l Novel Plim | 99.19%[c] | 98.22%[d] | 98.71% | 2.87102 | 2.6958 |

All calculations were based on *P*-value = 0.05.
**a**. CDW [g $l^{-1}$] = −30.29 + 4.989 Time.
**b**. PHA [%] = −10.23 + 2.929 Time.
**c**. CDW [g $l^{-1}$] = −15.50 + 4,317 Time − 12.17 Phosphorous [g $l^{-1}$].
**d**. PHA [%] = −18.93 + 3.324 Time + 7.16 Phosphorous [g $l^{-1}$].

 

feeding strategies, further regression models were calculated with addition of phosphate limitation as a stress factor for fermentation (see two bottom rows of Table 3). In both cases, results of $R^2_{adj.}$ were higher than in models without phosphate limitation.

Second phase of verification procedure was focussed on diagnosis of interdependencies of variables for most efficient fermentation, which is 20 l Novel Plim. First method used to analyse those relations was correlation coefficients (Table 4 and Fig. 4). All of tested variables had very high results of metrics (Time and CDW [g $l^{-1}$] $r = 0.995$; Time and PHA [%] $r = 0.989$; CDW [g $l^{-1}$] and PHA [%] $r = 0.975$) that confirms results of regression model. However, it is crucial to emphasize that adding phosphate limitation to the experiment results in a very high but negative correlation, both with CDW (−0.938) and with PHA (−0.889), that confirms its influence as a stress factor for fermentation.

Another way to verify interdependencies of variables of the experiment is Cronbach's alpha test. For all of the variables 20 l Novel Plim fermentation $\alpha = 0.7420$ and thus it is interpreted as acceptable consistency of factors. However, for phosphorous [g $l^{-1}$] in phosphate limited fermentation $\alpha = 0.8430$, that means good internal consistency of this variable within the model, and emphasis its influence on experiment.

**Table 4.** Correlation coefficient matrix for variables of fermentation 20 l Novel Plim with phosphate limitation as a stress factor.

| Variables | Time | CDW [g $l^{-1}$] | PHA [%] |
|---|---|---|---|
| CDW [g $l^{-1}$] | 0.995 | | |
| PHA [%] | 0.989 | 0.975 | |
| Phosphorous [g $l^{-1}$] | −0.921 | −0.938 | −0.889 |

## Conclusions

Mcl-PHA polymers have applications as elastomers in coatings, adhesives and a range of medical applications (Van Der Walle *et al.*, 1999; Guzik *et al.*, 2020). We report here a conversion technology of a complex mixture of fatty acids to achieve a cell dry weight (94.1 g $l^{-1}$) that is the highest in the literature for a fed-batch system without the addition of pure oxygen. Indeed, the strategy employed results in a PHA productivity that is comparable with the best reports for mcl-PHA production from single carboxylic acids (Lee *et al.*, 2000; Maclean *et al.*, 2008). The use of air rather than oxygen supplemented air significantly reduces the overall cost of the fermentation process.

Traditionally, optimization of bioprocesses took a largely trial and error form, which is costly, time-consuming and unpredictable (Maiti *et al.*, 2010). To streamline process improvement, mathematical models, when constructed properly, can be used to develop process understanding, design experimental plans and examine process scalability as was the aim here. From the outset, the model proved its worth *via* its effect on the standard operating procedure of fermentations. The construction and application of the mathematical model made it possible to determine the key variables and indicate existing multidimensional interdependencies. This study creates data and analytical tools that can be applied to bioprocess control for scale up of bacterial growth and PHA production.

In conclusion, a combination of microbiology, process engineering and statistical tools has been applied to develop a robust highly productive high yield process for the conversion of a mixture of fatty acids to the biodegradable polymer PHA.

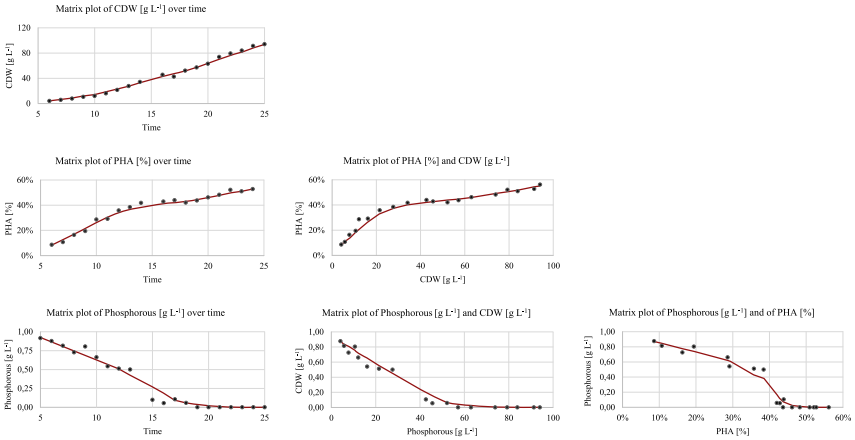


**Fig. 4.** Matrix plot for variables of fermentation 20 l Novel Plim with phosphate limitation.

 

## Experimental procedures

### *Bacterial growth medium*

The minimal mineral salts medium (MSM) contained per litre: 4.70 g $(NH_4)_2SO_4$, 3.00 g $MgSO_4 \times 7H_2O$, 15.00 g $Na_2HPO_4 \times 7H_2O$, 3.40 g $KH_2PO_4$ and trace elements as defined in Sun *et al.* (2007) and was used for all flask cultivations and fermentations carried out in this study. For phosphate limiting fermentations, the amount of $Na_2HPO_4 \times 7H_2O$ was reduced to 4.3 g $l^{-1}$, whereas $KH_2PO_4$ to 0.3 g $l^{-1}$. A synthetic fatty acid mixture (SFAM) containing fatty acids in range of butyric acid to tetradecanoic acid was supplied as the carbon and energy source for all feed development experiments (fatty acid origin Sigma Aldrich, Ireland; exact composition of fatty acids in SFAM in % vol/vol: butyric 8%, pentanoic 14%, hexanoic 13%, heptanoic 13%, octanoic 11%, nonanoic 11%, decanoic 10%, undecanoic 8%, dodecanoic 6%, tridecanoic 4%, tetradecanoic 2%; Fig. S1).

### *Inoculation culture conditions*

A culture of *Pseudomonas putida* KT2440 (Nogales *et al.*, 2008) was prepared by inoculating a single colony from *Pseudomonas* isolation agar (PIA) plates onto a fresh PIA plate. The culture was incubated at 30°C for 24 h. A loop of this culture was inoculated into 50 ml of MSM broth supplemented with 1.95 g of carbon per litre ($g_C$ $l^{-1}$) SFAM and incubated shaking at 250 rpm and 30°C between 12 and 16 h.

### *Fed-batch fermentation conditions*

Fed-batch fermentations were performed in a 5 l working volume Biostat B+ fermenter during model development and process improvement and a 20 l working volume Biostat C+ fermenter (Sartorius AG, Göttingen, Germany). Oxygen was supplied in the form of air (not supplemented with pure oxygen). The initial carbon source (SFAM) concentration was 0.84 $g_C$ $l^{-1}$ for the initial batch period.

Initial conditions for Biostat B+ fermentations (5 l) were as follows: starting volume –3 l; agitation – 500 rpm; aeration – 0 to 0.5 h no air due to rapid foam formation, thereafter 7 l $min^{-1}$; dissolved oxygen (DO) was controlled at 40% by increasing the agitation rate; pH was controlled automatically at 6.9 ± 0.1 by the addition of 20% $NH_4OH$ solution (Sigma, Arklow, Ireland) or 15% v/v $H_2SO_4$ (Sigma); foaming was controlled by the automatic addition of antifoam (polypropylene glycol P2000, Sigma) when required.

Initial conditions for Biostat C+ fermentations (20 l) were as follows: starting volume – 12 l; agitation – 300 rpm; aeration – 0 until 0.3 h no air due to rapid foam formation, there after 6 L $min^{-1}$; dissolved oxygen (DO) controlled at 20% by increasing the agitation and air flow rates (up to 30 l $min^{-1}$); pH was controlled automatically at 6.9 ± 0.1 by the addition of 20% $NH_4OH$ solution (Sigma) or 15% v/v $H_2SO_4$ (Sigma); foaming was controlled by the automatic addition of antifoam (polypropylene glycol P2000; Sigma) when required. DO was controlled at a lower level (20%) at 20 l scale fermentations. Data from each fermentation experiment were recorded by BioPAT® MFCS SCADA fermentation software (Sartorius AG).

### *Substrate supply*

There were four substrate feeding strategies applied during the course of this work.

*A simple exponential feeding strategy with a set specific growth rate.* After an initial batch phase (5 h), additional substrate was fed at the rate shown in Equation 1.

$$S_t = \frac{X_t}{Y_{X/S}} = \left(\frac{X_0}{Y_{X/S}}\right) e^{(\mu t)} \quad (1)$$

where $S_t$ is a total SFAM required to produce biomass $X_t$ at time $t$, $Y_{X/S}$ is the yield of biomass from the SFAM (0.80 g $g^{-1}$), $X_0$ is the initial biomass and $\mu$ is the desired specific growth rate.

*Substrate feeding based on a linearly decaying specific growth rate.* After an initial batch phase (5 h), substrate was fed to maintain a constant specific growth rate of 0.25 $h^{-1}$, in order to ensure that oxygen consumption will not become a limiting factor during the fermentation. This was continued until the cell dry weight reached ~ 3 g $l^{-1}$, at which point a feed rate designed to achieve a linearly decaying specific growth rate was imposed. The specific growth rate model was based on two parameters: $\mu_{init}$ – initial specific growth rate and $t_{max}$ – time over which the growth rate would decrease to zero. The imposed specific growth rate followed Equation 2, where $t$ was the time from the start of the decaying exponential growth, which was set at $t = 9$ h:

$$\mu = \frac{-\mu_{init}}{t_{max}} t + \mu_{init} \quad (2)$$

where $\mu_{init} = 0.25$ $h^{-1}$ with corresponding $t_{max} = 25$ h. Biomass concentration was expected to follow Equation 3, where $X_0$ was measured as 0.2 g. SFAM was fed according to Equation 4 to support this level of growth, based on the yield of biomass from SFAM, $Y_{X/S} =$ 0.8 g $g^{-1}$.

$$X_t = X_0 e^{\frac{-\mu_{init}}{2t_{max}} t^2 + \mu_{init} t} \quad (3)$$

 

$$S_t = \frac{X_t}{Y_{\frac{X}{S}}} = \frac{X_0 e^{\frac{-\mu_{\text{init}}}{2t_{\max}} t^2 + \mu_{\text{init}} t}}{Y_{\frac{X}{S}}} \quad (4)$$

*Substrate feeding based on a quadratically decaying specific growth rate.* After an initial batch phase, a feeding strategy designed to achieve a quadratically decaying specific growth rate was imposed (Maclean *et al.*, 2008). Similarly, to strategy 2 above, the specific growth rate model was based on two parameters: $\mu_{\text{init}}$ and $t_{\max}$. The imposed specific growth rate followed Equation 5, where $t$ was the time at which the quadratically decaying specific growth rate was imposed ($t = 5$ h):

$$\mu = \frac{-\mu_{\text{init}}}{t_{\max}^2} t^2 + \mu_{\text{init}} \quad (5)$$

where $\mu_{\text{init}} = 0.45\ \text{h}^{-1}$ with corresponding $t_{\max} = 25$ h. Parameters were set to achieve high productivity, while controlling $\mu X$ at a modest value (4 g $\text{i}^{-1}$ $\text{h}^{-1}$). This value was approximately 50% of the maximum productivity achievable as determined by the runs performed with a fixed specific growth rate of 0.25 $\text{h}^{-1}$. Biomass concentration was expected to follow Equation 6, where $X_0$ was measured as 0.2 g CDW. SFAM was fed according to Equation 7 to support this level of growth, based on the yield of biomass from SFAM, $Y_{X/S} = 0.8$ g $\text{g}^{-1}$.

$$X_t = X_0 e^{\frac{-\mu_{\text{init}}}{3t_{\max}^2} t^3 + \mu_{\text{init}} t} \quad (6)$$

$$S_t = \frac{X_t}{Y_{\frac{X}{S}}} = \frac{X_0 e^{\frac{-\mu_{\text{init}}}{3t_{\max}^2} t^3 + \mu_{\text{init}} t}}{Y_{\frac{X}{S}}} \quad (7)$$

This feed strategy continued until $\mu X$ achieved its set point (4 g $\text{l}^{-1}$ $\text{h}^{-1}$), at which time a constant rate of SFAM was fed to the system based on the $Y_{X/S} = 0.8$ g $\text{g}^{-1}$.

*A novel strategy developed for SFAM.* This strategy employs an initial exponential feeding stage (similar to that already described above), which aims to maintain the maximum specific growth rate. Using the model, it was determined how long this strategy could be maintained before the oxygen uptake rate (OUR) of the cells would exceed the maximum physical supply rate (as defined by reactor geometry, impeller speed, gassing rate, media properties etc.). In order to prolong the experiment and increase the biomass yield, the specific growth rate of the cells would have to be reduced in accordance with Equation 8:

$$OUR \propto \mu X \quad (8)$$

It can be seen that in order to keep OUR (oxygen uptake rate of the cells) constant while total biomass ($X$) is increasing, the specific growth rate ($\mu$) must fall. To reduce the growth rate and maintain a constant OUR (below the maximum supply rate), a suitable feed rate was imposed. The model was used to test a number of different rates, as it had to be high enough to achieve a reasonable productivity, but low enough to ensure the experiment could be extended for a suitable time period.

### *Statistical validation of the process*

First, a regression model was used to calculate the relationship between each of the dependent variables CDW [g $\text{l}^{-1}$] and PHA [%CDW] and two independent variables (time [h], phosphates concentration expressed as g of phosphorus per l [g $\text{l}^{-1}$]). In particular, linear regression and a fit regression model, based on calculating relationship between categorical and continuous predictors and one result, were applied. The next step of procedure focusses on diagnosing interdependencies of variable of the most efficient feeding strategy. Correlation coefficient and Cronbach's alpha test were applied. All calculations were made in the MiniTab 17 Statistical Software.

### *Other methods*

Other relevant methods and glossary of the abbreviations used in the text are available in the Supporting Information section, which include among others: nutrient and biomass analysis, downstream processing of biomass, PHA content and monomer composition determination from bacterial cultures, estimation of oxygen mass transfer coefficient ($k_La$) and detailed mathematical model development procedure.

## Conflict of interest

Authors declare no conflict of interest.

## Funding Information

This project has been funded under a grant from the Environmental Protection Agency of Ireland (2008-ET-LS-1-S2) and by the Ministry of Science and Higher Education within 'Regional Initiative of Excellence' Programme for 2019-2022. Project no.: 021/RID/2018/19. Total financing: 11 897 131,40 PLN. MG also acknowledges financial support from TechMatStrateg no. TECHMATSTRATEG2/407507/1/NCBR/2019.

## Author contributions

The manuscript was written through contributions of all authors. All authors have given approval to the final version of the manuscript.

 

## References


Babu, R.P., O'Connor, K., and Seeram, R. (2013) Current progress on bio-based polymers and their future trends. *Prog Biomater* **2:** 8.

Baldassarre, B., Calabretta, G., Bocken, N.M.P., and Jaskiewicz, T. (2017) Bridging sustainable business model innovation and user-driven innovation: a process for sustainable value proposition design. *J Clean Prod* **147:** 175–186.

Cardoso Diniz, S., Keico Taciro, M., Cabrera Gomez, J.G., and Da Cruz Pradella, J.G. (2004) High-cell-density cultivation of *Pseudomonas putida* IPT 046 and medium-chain-length polyhydroxyalkanoate production from sugarcane carbohydrates. *Appl Biochem Biotechnol - Part A Enzym Eng Biotechnol* **119:** 51–69.

Dias, J.M.L., Lemos, P.C., Serafim, L.S., Oliveira, C., Eiroa, M., Albuquerque, M.G.E., *et al*. (2006) Recent advances in polyhydroxyalkanoate production by mixed aerobic cultures: from the substrate to the final product. *Macromol Biosci* **6:** 885–906.

Drzyzga, O., Revelles, O., Durante-Rodríguez, G., Díaz, E., García, J.L., and Prieto, A. (2015) New challenges for syngas fermentation: towards production of biopolymers. *J Chem Technol Biotechnol* **90:** 1735–1751.

Fournet, M.B., Mcdonald, P., and Mojicevic, M. (2020) *Production of Polyhydroxybutyrate (PHB) and Factors Impacting Its Chemical and Mechanical Characteristics*.

Guzik, M., Witko, T., Steinbüchel, A., Wojnarowska, M., Sołtysik, M., and Wawak, S. (2020) What has been trending in the research of polyhydroxyalkanoates? A systematic review. *Front Bioeng Biotechnol* **8:** 959

Hartmann, R., Hany, R., Pletscher, E., Ritter, A., Witholt, B., and Zinn, M. (2006) Tailor-made olefinic medium-chain-length poly[(R)-3-hydroxyalkanoates] by *Pseudomonas* putida GPo1: batch versus chemostat production. *Biotechnol Bioeng* **93:** 737–746.

Lee, S.Y., Wong, H.H., Choi, J.I., Lee, S.H., Lee, S.C., and Han, C.S. (2000) Production of medium-chain-length polyhydroxyalkanoates by high-cell- density cultivation *Pseudomonas putida* under phosphorus limitation. *Biotechnol Bioeng* **68:** 466–470.

Maclean, H., Sun, Z., Ramsay, J., and Ramsay, B. (2008) Decaying exponential feeding of nonanoic acid for the production of medium-chain-length poly(3-hydroxyalkanoates) by *Pseudomonas putida* KT2440. *Can J Chem* **86:** 564–569.

Maiti, S.K., Singh, K.P., Lantz, A.E., Bhushan, M., and Wangikar, P.P. (2010) Substrate uptake, phosphorus repression, and effect of seed culture on glycopeptide antibiotic production: process model development and experimental validation. *Biotechnol Bioeng* **105:** 109–120.

Moradali, M.F., and Rehm, B.H.A. (2020) Bacterial biopolymers: from pathogenesis to advanced materials. *Nat Rev Microbiol* **18:** 195–210.

Narancic, T., Verstichel, S., Reddy Chaganti, S., Morales-Gamez, L., Kenny, S.T., De Wilde, B., *et al*. (2018) Biodegradable plastic blends create new possibilities for end-of-life management of plastics but they are not a panacea for plastic pollution. *Environ Sci Technol* **52:** 10441–10452.

Nitkiewicz, T., Wojnarowska, M., Sołtysik, M., Kaczmarski, A., Witko, T., Ingrao, C., and Guzik, M. (2020) How sustainable are biopolymers? Findings from a life cycle assessment of polyhydroxyalkanoate production from rapeseed-oil derivatives. *Sci Total Environ* **749:** 141279.

Nogales, J., Palsson, B., and Thiele, I. (2008) A genome-scale metabolic reconstruction of *Pseudomonas putida* KT2440: iJN746 as a cell factory. *BMC Syst Biol* **2:** 79.

Salmiati, Ujang, Z., Salim, M.R., Md Din, M.F., and Ahmad, M.A. (2007) Intracellular biopolymer productions using mixed microbial cultures from fermented POME. *Water Sci Technol* **56:** 179–185. https://doi.org/10.2166/wst.2007.687.

Sun, Z., Ramsay, J.A., Guay, M., and Ramsay, B.A. (2007) Carbon-limited fed-batch production of medium-chain-length polyhydroxyalkanoates from nonanoic acid by *Pseudomonas putida* KT2440. *Appl Microbiol Biotechnol* **74:** 69–77.

Tobin, K.M., McGrath, J.W., Mullan, A., Quinn, J.P., and O'Connor, K.E. (2007) Polyphosphate accumulation by *Pseudomonas putida* CA-3 and other medium-chain-length polyhydroxyalkanoate-accumulating bacteria under aerobic growth conditions. *Appl Environ Microbiol* **73:** 1383–1387.

Van Der Walle, G.A.M., Buisman, G.J.H., Weusthuis, R.A., and Eggink, G. (1999) Development of environmentally friendly coatings and paints using medium-chain-length poly(3-hydroxyalkanoates) as the polymer binder. *Int J Biol Macromol* **25:** 123–128.


## Supporting information

Additional supporting information may be found online in the Supporting Information section at the end of the article.

**Fig. S1**. Synthetic fatty acid mixture (SFAM) used for cultivation of bacteria in this study.

**Fig. S2**. Feed profiles for fed batch fermentations in Biostat B+ fermentor using SFAM. Linear – linearly decreasing growth rate feed profile (adapted from (Maclean et al., 2008)); Quadratic – quadraticly decaying growth rate feed profile (adapted from (Maclean et al., 2008)); Hybrid – a novel feed profile developed in this study.

**Fig. S3**. Growth of *P. putida* KT2440 on SFAM fed according to a linearly decaying specific growth rate. Cell dry weight (CDW) (g $L^{-1}$,▲), $NH_4^+$ concentration (g $L^{-1}$,●) and dissolved oxygen (%, ○) were tracked over time. The experimental data was compared to model predictions (corresponding lines).

**Fig. S4**. Growth of *P. putida* KT2440 on SFAM fed according to a quadratically decaying specific growth rate. Cell dry weight (CDW) (g $L^{-1}$,▲), $NH_4^+$ concentration (g $L^{-1}$,●) and dissolved oxygen (%, ○) were tracked over time. The experimental data was compared to model predictions (corresponding lines).

**Fig. S5**. Comparison of PHA accumulation profiles for non-limiting (Panel A) and phosphate limiting (Panel B) conditions. Visible two distinct phases in both fermentation types: a) 1st stage – in both types of fermentation bacteria

accumulate PHA to ~ 40% exponentially; b) 2nd stage – in a non-limiting experiment PHA accumulation stagnates at ~ 30%–40%, whereas in the phosphate limiting experiment bacteria continue to accumulate PHA linearly. Imposing phosphate limitation aids in continuation of PHA accumulation visible as an up-trend of the second phase (purple squares).

**Table S1**. Monomer composition of PHA accumulated by P. putida KT2440 grown under various conditions.

 